The Location of Hysteresis Phenomena in Rochelle Salt Crystals

W. P. MASON
Bell Telephone Laboratories, New York, New York
(Received August 12, 1940)

Measurements of the elastic properties of an unplated crystal, the piezoelectric constant f_{14}, and the clamped dielectric constant of a Rochelle salt crystal show that practically all hysteresis and dissipation effects are associated with the clamped dielectric properties of the crystal. A theoretical formulation of the equations of a piezoelectric crystal has been made which takes account of the dissipation effects. The formulation is given for the polarization theory. The frequency variation of the clamped dielectric constant when interpreted by Debye's theory of dielectrics, modified to take account of hysteresis losses, indicates that there are two components, one of which has associated with it at high viscous resistance, whereas the other one does not. The nonviscous component has a dielectric constant of about 100 at 0°C and is probably due to the displacement of the ions in the lattice structure. The viscous component has a dielectric constant of about 140 at 0°C and is probably due to the dipoles of the Rochelle salt. Both components have higher dielectric constants and hysteresis between the Curie points indicating a cooperative action of the molecules for both components in this temperature region.

I. INTRODUCTION

IT has been pointed out in several recent papers[1,2,3] that the large changes, with temperature, of the dielectric constant, the elastic constant, and the piezoelectric constant d_{14} of a fully plated Rochelle salt crystal are due, fundamentally, to the variation of the clamped dielectric constant of the crystal with temperature. It is the purpose of the present paper to show that the large dissipation associated with the motion of a Rochelle salt crystal is also due practically entirely to the hysteresis and viscous resistance associated with the elements contributing to the clamped dielectric constant and is not associated with the elastic motion of the lattice elements of the crystal or with the piezoelectric constant f_{14} which determines the ratio between mechanical force applied to the crystal lattice and the electrical polarization of the crystal.

At low frequencies the principal effect of dissipation is to produce large hysteresis loops in the charge-potential curve as shown by Fig. 1, taken from a paper by Mueller.[4] When the crystal is prevented from moving by applying an external force to it, the magnitude of the dielectric constant and hence the charge through the crystal becomes less as shown by Fig. 1. This follows from the fact that, as the motion of the lattice is inhibited, the additive polarization produced by this motion is eliminated and hence the charge does not rise to so high a value. Cutting down the additive polarization also cuts down the size of the hysteresis loop.

When the impedance of a vibrating crystal is measured near its resonant region, the effect of the dissipation is shown by the finite value of the resistance at the resonant frequency of the crystal. In a former paper,[1] the resonant and antiresonant frequencies of a 45° X-cut crystal having the dimensions, length = 2.014 cm; width = 0.418 cm; thickness = 0.104 cm were measured as a function of the temperature and were plotted on Fig. 1 of that paper. At the same time the resistance at resonance was measured. The complete data are given in Table I.

II. LOCATION OF HYSTERESIS EFFECT

The source of the large dissipation in X-cut Rochelle salt crystals, might conceivably lie in a mechanical hysteresis of the motion of the crystal lattice, in a hysteresis or lag in the piezoelectric constant, or in the clamped dielectric constant. In order to determine which source was causing

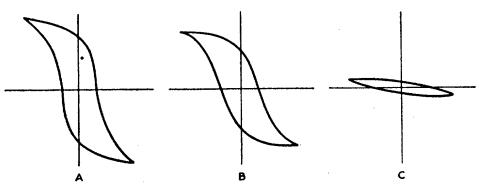

FIG. 1. The change of the hysteresis curve of Rochelle salt with pressure ($t=0°$). (1) free crystal, (2) pressure 1 kg/cm² on both sides, (3) pressure 7 kg/cm² on both sides. Maximum field 2 kv/cm.

[1] W. P. Mason, Phys. Rev. **55**, 775 (1939).
[2] A. N. Holden and W. P. Mason, Phys. Rev. **57**, 54 (1940).
[3] H. Mueller, Phys. Rev. **57**, 829 (1940).
[4] H. Mueller, Phys. Rev. **47**, 175 (1935).

the hysteresis effect, measurements were made of each of the properties of the crystal separately. To measure the mechanical properties separately it is necessary to measure the elastic properties of a bare crystal without plating since, as shown in two former papers,[1,3] in an unplated crystal the piezoelectric properties are eliminated. The elastic constant of a 45° X-cut crystal was measured and shown in the data of Table I, f_M, by measuring such a crystal between widely spaced electrodes. It was desired however, to measure the dissipation also and this is difficult by this method. The method used here was to glue an approximately half-wave-length unplated Rochelle salt crystal to a half-wave-length quartz crystal and measure the change in resonance frequency and measured resistance of the quartz crystal caused by the added Rochelle salt crystal. This method used originally by Quimby and Balamuth[5] has been used widely to measure the elastic constants and internal dissipation of many metals. The frequency constant is measured by the change in frequency of the quartz crystal, while the internal resistance is measured by the change in resistance of the crystal at the resonant frequency. Then, knowing the density of the specimen measured, all the elastic properties can be determined. As shown by Eqs. (47) of the next section, the impedance of such a specimen near its half-wave-length frequency can be regarded as equivalent to that of a series resistance, mass, and compliance, and the internal dissipation can best be expressed as a ratio q of the reactance of one of these elements at the resonant frequency to the resistance at resonance. Figure 3 shows a measurement of the frequency constant f_M and the q of an X-cut crystal with its length 45° from the Y and Z axes, having the dimensions $L=2.015$ cm; $W=0.4$ cm; $T=0.1$ cm. The values of f_M agree well with those given on Table I. The q of the crystal is high outside the Curie region except above 40°C when the crystal is approaching its melting point. Inside the limits of the Curie points, the q is appreciably lower.

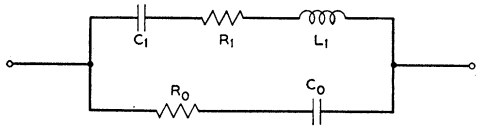

FIG. 2. Equivalent electrical circuit of longitudinally vibrating crystal. C_0 and R_0 are capacitance and resistance associated with the longitudinally clamped dielectric constant. C_1 R_1 and L_1 are the capacitance, resistance and inductance associated with the motional properties of the crystal.

If the piezoelectric stress is proportional to the polarization it has been shown by Mueller,[3] that the elastic constant of a bare or unplated crystal depends somewhat on the piezoelectric constant and the dielectric properties of the crystal. The question arises whether the measured lowering of the q and frequency constant between the Curie points, where the piezoelectric effect is high, can be due to this interaction. The question is considered theoretically in the next section, and it is there shown that the theoretical change in the complex elastic constant is much too small to account for the measured results. We conclude, therefore, that between the two Curie points a small but definite change takes place in the elastic constants of the crystal.[6]

TABLE I. *Resonant and antiresonant frequencies of a 45° X-cut crystal. In this table f_R is the resonant frequency and f_A the antiresonant frequency of the fully plated crystal, f_M the frequency of the same crystal per cm without plating and R_E the electrical resistance of the crystal at the resonant frequency. The fifth column shows the coefficient of electromechanical coupling as defined previously or in this paper, while the sixth column shows the ratio q of reactance to resistance of the motional impedance of the crystal. This is found by taking the reactance of the coil of the equivalent circuit of the crystal shown on Fig. 2, and dividing by the measured resistance.*

T°C	f_R	f_A	Resistance R_E at resonance in ohms	f_M constant kc per cm	Coefficient of coupling k	q
−12°	72,210	96,700	—	216,890	73.9	
−10.5	77,600	98,510	—		69.1	
− 9	79,100	99,510	1300	216,550	67.5	16.8
− 5	82,660	100,790	1800		63.5	16.5
− 3	83,950	100,820	—		61.9	
+ 1	84,450	100,830	2400	215,220	61.0	14.0
5	84,200	100,630	2600		61.0	13.7
9	83,750	100,250	2500	214,000	61.0	14.0
13.0	81,840	99,850	2400		63.2	13.9
15.0	80,400	99,220	2200	212,890	64.8	12.3
16.5	79,200	98,710	1800		66.0	13.7
17.5	78,410	97,700	1500		66.8	15.0
20.5	71,820	95,200	900	212,220	73.0	16.3
22.7	61,600	90,420	430		80.9	20.9
23.7	56,120	84,130	200	211,440	84.5	31.1
24.7	52,000	81,600	60	212,200	87.5	101.0
25.7	64,130	91,110	65	212,000	79.0	152.0
28.2	74,710	96,220	60	211,440	70.0	312.0
31.0	82,550	99,000	65		61.0	550.0
34.2	86,700	100,100	70	211,000	55.0	820.0
38.0	90,200	100,610	120		49.0	845.0
40.2	91,120	100,650	250	208,780	47.0	490.0
42.0	92,630	100,750	410		44.0	389.0
47.5	94,150	100,900	2250	207,120	40.0	97.5

[5] L. A. Balamuth, Phys. Rev. **45**, 715 (1934).

[6] This change in the complex elastic constant is probably related to the spontaneous deformation observed by Mueller.[3] This would cause a slight change in the lattice spacings and hence a slight change in the elastic constant between the Curie points.

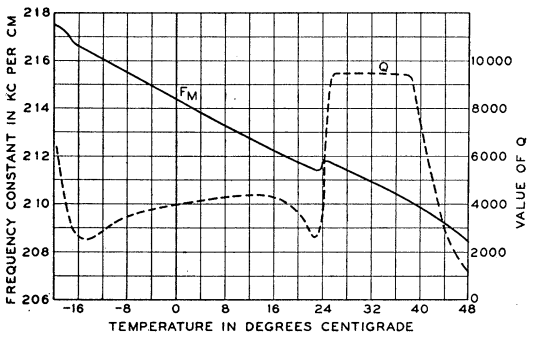

FIG. 3. Measurement of the frequency constant and the ratio q of reactance to resistance for mechanical motion of an unplated 45° X-cut Rochelle salt crystal.

It can be shown theoretically that, if all other sources of dissipation are small compared to the elastic dissipation, the electrical q of a crystal as shown on Table I will be equal to the mechanical q as measured on Fig. 3. The fact that the electrical q is much lower, shows that mechanical hysteresis plays a negligible part in the hysteresis loops observed for low frequency measurements, or the low electrical q's measured on Table I.

We next consider the possibility of hysteresis effects in the piezoelectric stress-polarization relationships. This requires measuring directly the piezoelectric constant f_{14} which relates piezoelectric stress to the polarization in the absence of a strain in the crystal, or the voltage generated in the crystal by a given strain in the absence of a charge on the surface. The latter proportionality is the easier to measure for it can be measured by comparing the open circuit voltage generated by a 45° X-cut Rochelle salt crystal with the open circuit voltage generated for a quartz crystal when both are subject to known relative strains. The experimental method of accomplishing this is shown on Fig. 4. We have a long longitudinally vibrating quartz crystal, with the plating divided into two parts, as shown on Fig. 4, glued to a 45° X-cut Rochelle salt crystal with a small amount of plating at its center. The first pair of plates are attached to an oscillator which drives the crystal at the frequency of its second harmonic vibration. The length of the Rochelle salt crystal is adjusted so that it is half a wave-length at the second harmonic resonant frequency of the crystal. The voltage gathering electrodes cover only a small part of the quartz or Rochelle salt crystals and are located at a node of the motion where the strain is a maximum and is uniform for some distance on either side of the node since it follows a cosine law. The voltages generated by each crystal are connected alternately to a very high impedance detector and compared in magnitude. Since the glued joint between the Rochelle salt and the quartz comes at a loop in the motion very little strain is placed on it and hence the displacement of the glued quartz edge is the same as that for the glued Rochelle salt edge. Since the length of the section of the quartz bar used for pick-up is somewhat longer than that of the Rochelle salt bar, it is evident that the Rochelle salt bar will be somewhat more strained than the quartz bar. It can be shown theoretically that the strain at the centers of the two bars are opposite in sign and equal, respectively, to the ratio

$$y_{y_R}/y_{y_q} = -V_q/V_R = -509/420 = -1.212 \quad (1)$$

for the quartz and Rochelle salt cuts used, where V_q and V_R are, respectively, the velocity of propagation in quartz and Rochelle salt and y_{yR} and y_{yq} are the strains in the Rochelle salt and quartz bars, respectively.

It is shown in the next section, Eq. (26), that the open circuit voltage developed in the Rochelle salt bar is

$$E_R \doteq f_{14} l_t y_y / 2c_{44} s_{22}', \quad (2)$$

where f_{14} is the piezoelectric constant, c_{44} the shear modulus, s_{22}' the inverse of Young's modulus along the length of the crystal, and l_t the thickness of the crystal. Similarly, the open circuit voltage for quartz is

$$E_Q = 4\pi d_{12}' y_y l_t / K s_{22}' = 1.312 \times 10^5 l_t y_y \quad (3)$$

for the quartz crystal used. This was a −18.5° X-cut crystal[7] and the measured constants were

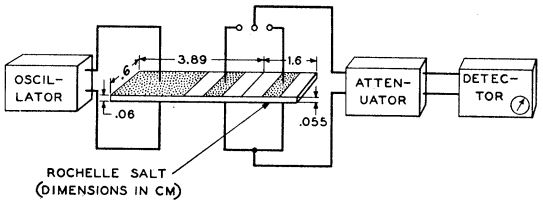

FIG. 4. Circuit and apparatus for measuring the piezoelectric constant f_{14} of Rochelle salt.

[7] This crystal is described in "Electrical wave filters employing quartz crystals as elements," W. P. Mason, Bell Sys. Tech. J. (July, 1934) Appendix 1.

$d_{12}' = 6.91 \times 10^{-8}$; $K = 4.55$; $s_{22}' = 1.455 \times 10^{-12}$. On account of the small capacitance of the quartz element, not all of this voltage appeared across the output for, because of the distributed capacitance around the crystal, an attenuation of voltage occurred. As near as could be determined the static capacitance of the crystal was 3.25 $\mu\mu$f while the distributed capacitance was 2.75 $\mu\mu$f, giving a measured voltage of

$$E_q = 7.11 \times 10^4 \, l_t y_y. \quad (4)$$

On account of the large capacitance inherent in the Rochelle salt element, about 90 $\mu\mu$f, this source caused no appreciable error in the Rochelle salt voltage. When the two voltages were compared it was found that at 30°C the Rochelle salt crystal voltage was 1.41 times as large as the quartz voltage. This gives the value for f_{14} equal to

$$f_{14} = 2c_{44}s_{22}'(l_{t_Q}/l_{t_R}) \times (y_{y_Q}/y_{y_R}) \times 1.41 \times 7.11 \times 10^4 = 7.58 \times 10^4 \quad (5)$$

upon inserting the values of the constants measured previously[1] for Rochelle salt.

While on account of the difficulty of measuring the distributed capacitance of the quartz bar, the absolute value given by this method is not very accurate, the relative values obtained over a wide temperature range are very accurate since the distributed capacitance remains constant at all temperatures. Accordingly the value of f_{14} was measured over a wide temperature range with the results shown on Fig. 5. It appears that the constant f_{14} is an absolute constant of the material and does not change with temperature.

The phase angle of the constant could be determined by measuring the relative phases of the quartz generated voltage and the Rochelle salt generated voltage. This, however, is a difficult experiment to perform and has not been attempted here. The fact that f_{14} has a negligible phase angle however is shown by the measurements discussed below.

Since it can be shown that there is no appreciable lag or hysteresis with respect to either the elastic constant or piezoelectric constant, it appears that all of the hysteresis and dissipation must be associated with the clamped dielectric constant. In order to verify this, it is desirable to

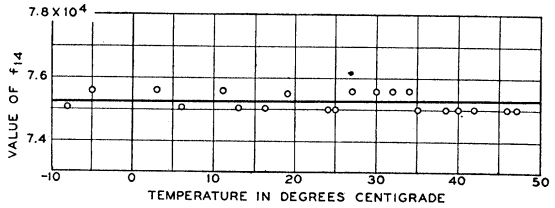

FIG. 5. Measurement of the piezoelectric constant f_{14} over a wide temperature range.

measure the dielectric constant and the associated resistance of the clamped crystal. On account of the difficulty of clamping a crystal so that no strain occurs, this cannot be completely accomplished. If, however, we use a long, thin, longitudinally vibrating crystal and measure its impedance at twice the longitudinal resonance frequency of the plated crystal, a very similar result will be obtained. This follows from the fact that, at twice the natural longitudinal resonance, half the crystal will be compressed and the other half extended so that the charge contributed by the piezoelectric effect will be zero for a crystal which has a continuous plating over the whole surface. This condition is discussed in more detail in the next section and it is there shown that what will be measured is essentially a resistance R corresponding to the resistance associated with the clamped crystal in series with a capacitance determined by the dielectric constant K_{LC}, which is related to the clamped dielectric constant K by the equation

$$\frac{4\pi}{K_{LC}} \doteq \frac{4\pi}{K} - \frac{f_{14}^2}{c_{44}}\left(1 - \frac{1}{4c_{44}s_{22}'}\right) = \frac{4\pi}{K} - 0.0179, \quad (6)$$

introducing the measured values into this equation.

To obtain the dielectric dissipation, a crystal having the dimensions, length = 4.03 cm; width = 0.8 cm; thickness = 0.2 cm was obtained, i.e., with all dimensions twice those of the crystal of Table I, and the electrical impedance of the crystal was measured at the frequencies corresponding to the temperatures of Table I. The results translated into dielectric constant and series resistance in ohms per cubic cm are shown on Fig. 6 by the solid lines. It is evident that considerable dielectric dissipation is obtained particularly between the Curie points. Above 40°C, the dissipation again increases because of the

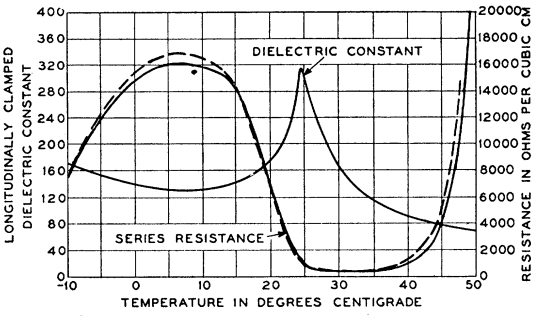

FIG. 6. Measurement of the longitudinally clamped dielectric constant and associated series resistance of a 45° X-cut crystal.

increase in leakage resistance as the crystal approaches its melting point. This increase agrees with the increase that can be obtained by direct current measurements.

If all the dissipation associated with the crystal is concentrated in the clamped dielectric constant, it is shown in the next section that the electrical resistance of a vibrating crystal measured at the resonant frequency will be

$$R_E=\pi^2 l_t R/8 l_w l_y, \tag{7}$$

where R is the dielectric resistance per cubic centimeter associated with the clamped dielectric constant which has been measured as shown on Fig. 6. To test this relationship, we can make use of the measured electrical resistance R_E of Table I. This resistance multiplied by the factor

$$\frac{l_w l_y}{l_t}\frac{8}{\pi^2}=\frac{0.418\times 2.014\times 8}{0.104\times 9.89}=6.63 \tag{8}$$

is shown plotted by the dotted lines of Fig. 6. The good agreement between this curve and the solid line curve of the dielectric dissipation is a proof that practically all the dissipation in the crystal is located in the clamped dielectric constant. All of these measurements were made for low voltages, i.e., less than 5 volts per cm. Since it is shown in the last section that the resistances measured were largely due to hysteresis, the question arises as to whether these resistances will vary with the voltage applied. This was tested over a 30 to 1 voltage range by measuring the resistance R_E at resonance, and it was found that the variation was very small indicating that the areas of the hysteresis loops for low charge densities were approximately proportional to the square of the applied charge or voltage.

III. Theoretical Formulation of the Equations of Motion Taking Account of Dissipation

Equations for piezoelectric crystals have been obtained by assuming that the piezoelectric stress is proportional to the potential gradient (Voigt), internal electric field (Mueller, 1935), charge density on the electrodes (Mason), or polarization (Mueller, 1940). When one measures the elastic, electric, and piezoelectric constants of a Rochelle salt crystal over a wide temperature range, he finds that all of the elastic, piezoelectric and dielectric constants vary widely with temperature, plating condition, etc., on the basis of the first two theories. Under the last two theories, the elastic and piezoelectric constants are entirely normal and vary little with temperature, while the clamped dielectric constant has a temperature variation entirely consistent with the cooperative phenomenon existing among the molecules of the crystal. For this reason the latter two theories are to be preferred.

Because of the high dielectric constant in Rochelle salt, these two theories give results identical within less than one percent.[8] If, however, we regard the piezoelectric effect as an internal phenomenon, as is usually done, the polarization formulation is theoretically correct and will be followed here. If the force is proportional to the polarization, Mueller has shown that to the elastic constant $1/c_{44}$ one has to add a small quantity $f_{14}^2/4\pi c_{44}^2$ which is usually less than 0.3

[8] H. Mueller (reference 3 footnote 21) has objected to the theoretical results given in reference 1. In this he appears to be incorrect, for substantially the same results are obtained with the equations of reference 1. With the set of data given in Table II of reference 3, and a value of $c_{44}=11.6\times 10^{10}$ the value of $f_{14}=7.2\times 10^4$. From the same data and the theoretical formulation given in reference 1, the result is $f_{14}=7.2\times 10^4$. A comparison of the d_{14} constant as defined by Voigt for the two methods is shown below.

t°C	d_{14} (Mueller)	d_{14} (Mason)
24.7	67.7×10^{-6}	67.4×10^{-6}
25.7	37.2	37.4
28.2	20.6	20.6
31.0	12.8	12.8
34.2	9.1	9.2
38.0	6.65	6.57
40.2	5.88	6.05
42.0	5.07	5.00
47.5	4.0	3.92

percent of $1/c_{44}$. The effect on the dissipation is more marked as is shown in this section. The measurements of the complex elastic constant given in Fig. 3 show that between the Curie points the dissipation of the unplated crystal is considerably higher than outside this range. To see if the polarization theory can account for this effect without assuming a change in the elastic constants, the formulation of the polarization theory taking account of dissipation is given in this section.

The free energy per cubic centimeter Φ of the crystal can be written for Rochelle salt in the form

$$\begin{aligned}\Phi=&\tfrac{1}{2}(c_{11}x_x^2+c_{22}y_y^2+c_{33}z_z^2+c_{44}y_z^2+c_{55}z_x^2+c_{66}x_y^2)\\&+(c_{12}x_xy_y+c_{13}x_xz_z+c_{23}y_yz_z)\\&+(f_{14}y_zP_x+f_{25}z_xP_y+f_{36}x_yP_z)\\&+\tfrac{1}{2}(\chi_1P_x^2+\chi_2P_y^2+\chi_3P_z^2),\end{aligned}\quad(9)$$

where P_x, P_y, P_z are the components of the polarization, x_x, $\cdots$, y_z are the strains in the crystal, c_{ik} are the elastic constants of the crystal, f_{ik} are the piezoelectric constants of the crystal, and χ_i are the reciprocals of the electric susceptibilities of the clamped crystal, i.e., free from strain.

By differentiation with respect to the strains we obtain the stresses ($-X_x=\partial\Phi/\partial x_x$) while the field strength (potential gradients) are given by $E_x=\partial\Phi/\partial P_x$. This will furnish nine equations, three each of the following type

$$\begin{aligned}-X_x&=c_{11}x_x+c_{12}y_y+c_{13}z_z,\\-Y_z&=c_{44}y_z+f_{14}P_x,\\E_x&=f_{14}y_z+\chi_1P_x.\end{aligned}\quad(10)$$

It was shown in the previous section that practically all the dissipation associated with the motion of a Rochelle salt crystal was associated with dissipation of the clamped dielectric constant. If all this dissipation is of the viscosity type, i.e., determined by the rate of change of polarization, the resulting equation can be determined from a dissipation function of the type

$$F=\tfrac{1}{2}(R_{v1}\dot{P}_x^2+R_{v2}\dot{P}_y^2+R_{v3}\dot{P}_z^2).\quad(11)$$

Then from Lagrange's generalized equations, the last of Eqs. (10) becomes

$$\begin{aligned}E_x&=f_{14}y_z+\chi_1P_x+R_{v1}\dot{P}_x\\&=f_{14}y_z+(\chi_1+j\omega R_{v1})P_x\end{aligned}\quad(12)$$

for simple harmonic motion.

A dissipation function of the type shown by Eq. (11) cannot represent a hysteresis effect, for at a slow rate of change of polarization, the effect of the resistance R_{v1} disappears. In fact a hysteresis effect is strictly a nonlinear effect and cannot be represented by any linear dissipation function. By analogy with the same effect occurring in iron core coils, however, a hysteresis effect can be represented as far as bridge, current, or other measurements which average the result of a complete cycle, by a resistance which varies inversely as the frequency. The energy loss per cycle is the area of the charge-potential loops of the type shown on Fig. 1, while the power loss is this area multiplied by the frequency or

$$P_L=\text{area}\cdot f=Af.\quad(13)$$

The power loss in a resistance R_H required to represent this loss is

$$P_L=R_H\dot{P}_x^2.\quad(14)$$

Hence

$$R_H=\frac{Af}{\dot{P}_x^2}=\frac{Af}{4\pi^2f^2P_x^2}=\frac{A}{4\pi^2f\kappa_1^2E_x^2},\quad(15)$$

where κ_1 is the susceptibility of the condenser.

If we introduce this value into Eq. (12) we have

$$\begin{aligned}E_x=f_{14}y_z+[\chi_1+j\omega(R_H+R_v)_1]P_x=f_{14}y_z\\+(\chi_1+j\omega R_1)P_x=f_{14}y_z+\chi_{1c}P_x,\end{aligned}\quad(16)$$

where R_1 represents the combined effect of the hysteresis and viscosity resistances and χ_{1c} denotes the complex quantity $(\chi_1+j\omega R_1)$.

In measuring the constants of a crystal with a field applied along the X axis by dynamic means, a longitudinal vibration of a long thin crystal with its length 45° from the Y and Z axis is usually employed. The equations of use for an X-cut crystal are

$$\begin{aligned}-X_x&=c_{11}x_x+c_{12}y_y+c_{13}z_z,\\-Y_y&=c_{12}x_x+c_{22}y_y+c_{23}z_z,\\-Z_z&=c_{13}x_x+c_{23}y_y+c_{33}z_z,\\-Y_z&=c_{44}y_z+f_{14}P_x,\\E_x&=(\chi_1+j\omega R_1)P_x+f_{14}y_z.\end{aligned}\quad(17)$$

By solving this set of linear equations we can also express the equations in the form

$$\begin{aligned} -x_x &= s_{11}X_x + s_{12}Y_y + s_{13}Z_z, \\ -y_y &= s_{12}X_x + s_{22}Y_y + s_{23}Z_z, \\ -z_z &= s_{13}X_x + s_{23}Y_y + s_{33}Z_z, \\ -y_z &= s_{44}Y_z + d_{14}E_x, \\ P_x &= d_{14}Y_z + \kappa_1 E_x, \end{aligned} \tag{18}$$

where $s_{11}=\Delta_{11}/\Delta$; $s_{23}=\Delta_{23}/\Delta$, etc., where Δ is the determinant

$$\Delta = \begin{vmatrix} c_{11} & c_{12} & c_{13} \\ c_{12} & c_{22} & c_{23} \\ c_{13} & c_{23} & c_{33} \end{vmatrix}, \tag{19}$$

and Δ_{11} is the determinant obtained from this by suppressing the first row and first column. Similarly

$$d_{14}=f_{14}/D; \quad s_{44}=(\chi_1+j\omega R_1)/D; \quad \kappa_1=c_{14}/D,$$

$$\text{where} \qquad D=c_{44}(\chi_1+j\omega R_1)-f_{14}^2. \tag{20}$$

The s_{11}, s_{12}, s_{13}, s_{22}, s_{23}, s_{33} constants are the compliances of the crystal which can be measured by mechanical means when the crystal is plated or unplated. The compliance s_{44} is the compliance of the crystal when $E_x=0$ or when the crystal is plated and short circuited. Similarly d_{14} is the ratio of the strain to the applied field when $Y_z=0$ or the crystal is free to move, and κ_1 is the susceptibility of the crystal when $Y_z=0$ or the crystal is free to move. We note that the three constants s_{44}, d_{14}, and κ_1 involve a resistive component and, hence, will show hysteresis effects when measured statically. Since c_{44}, f_{14}, and χ_1 do not involve the state of elastic deformation, and only one of them shows hysteresis effects, we regard these as the true constants of the crystal and shall use them in further calculations.

We note first that if the crystal is free to vibrate, which happens when $Y_z=0$, that

$$y_z=-\frac{f_{14}}{c_{44}}P_x$$

and hence

$$E_x=[\chi_1-f_{14}^2/c_{44}+j\omega R_1]P_x, \tag{21}$$

$\chi_1-f_{14}^2/c_{44}=\chi_F$, where χ_F is the inverse of the susceptibility of a free crystal. Hence, we see that if all the dissipation is concentrated in the clamped dielectric constant, one should measure the same resistance R_1 whether the crystal is prevented from moving or not.

In calculating the motion of the rotated crystal, it is desirable to obtain the constants of the rotated crystal. This can be done by means of the transformations given in reference 1 appendix I. For the crystal cut perpendicular to the X axis and rotated so that its length, designated the Y' axis is 45° from the Y and Z axes, the equations become

$$\begin{aligned} -X_x &= c_{11}x_x + \tfrac{1}{2}(c_{12}+c_{13})y_y' + \tfrac{1}{2}(c_{12}+c_{13})z_z' \\ &\quad + \tfrac{1}{2}(c_{13}-c_{12})y_z', \\ -Y_y' &= \tfrac{1}{2}(c_{12}+c_{13})x_x + \tfrac{1}{4}(c_{22}+c_{33}+2c_{23}+4c_{44})y_y' \\ &\quad + \tfrac{1}{4}(c_{22}+c_{33}+2c_{23}-4c_{44})z_z' \\ &\quad + \tfrac{1}{4}(c_{33}-c_{22})y_z' + f_{14}P_x, \\ -Z_z' &= \tfrac{1}{2}(c_{12}+c_{13})x_x + \tfrac{1}{4}(c_{22}+c_{33}+2c_{23}-4c_{44})y_y' \\ &\quad + \tfrac{1}{4}(c_{22}+c_{33}+2c_{23}+4c_{44})z_z' \\ &\quad + \tfrac{1}{4}(c_{33}-c_{22})y_z' - f_{14}P_x, \\ -Y_z' &= \tfrac{1}{2}(c_{13}-c_{12})x_x + \tfrac{1}{4}(c_{33}-c_{22})y_y' \\ &\quad + \tfrac{1}{4}(c_{33}-c_{22})z_z' + \tfrac{1}{4}(c_{22}+c_{33}-2c_{23})y_z', \\ E_x &= (\chi_1+j\omega R_1)P_x + f_{14}(y_y'-z_z'). \end{aligned} \tag{22}$$

Solving these equations by letting $X_x=Z_z'=Y_z'=0$ we find

$$\begin{aligned} -Y_y' &= y_y'\left[\frac{4}{1/c_{44}+s_{22}+s_{33}+2s_{23}}\right] \\ &\quad + \frac{f_{14}P_x}{2c_{44}}\left[\frac{4}{1/c_{44}+s_{22}+s_{33}+2s_{23}}\right], \\ E_x &= P_x\left[\chi_1+j\omega R-\frac{f_{14}^2}{c_{44}}\left(\frac{s_{22}+s_{33}+2s_{23}}{1/c_{44}+s_{22}+s_{33}+2s_{23}}\right)\right] \\ &\quad + \frac{f_{14}y_y'}{2c_{44}}\left[\frac{4}{1/c_{44}+s_{22}+s_{33}+2s_{23}}\right]. \end{aligned} \tag{23}$$

We designate

$$\chi_1-\frac{f_{14}^2}{c_{44}}\left(\frac{s_{22}+s_{33}+2s_{23}}{1/c_{44}+s_{22}+s_{33}+2s_{23}}\right)=\chi_{LC}, \tag{24}$$

indicating that it is the inverse of the susceptibility measured when the crystal is longitudinally clamped, i.e., prevented from moving along the length but not along the width or thickness. This is a measurable quantity as shown in section II. We have, also, that

$$\tfrac{1}{4}(1/c_{44}+s_{22}+s_{33}+2s_{23})=s_{22}', \tag{25}$$

the true elastic compliance along the direction of the length of the crystal.

With these values, Eqs. (23) become

$$-Y_y'=\frac{y_y'}{s_{22}'}+\frac{f_{14}P_x}{2c_{44}s_{22}'};$$

$$E_x=P_x[\chi_{LC}+j\omega R_1]+\frac{f_{14}y_y'}{2c_{44}s_{22}'}. \tag{26}$$

To these we add another equation relating the charge on the surface per unit area of the crystal to the voltage and polarization, namely,

$$Q=E_x/4\pi+P_x. \tag{27}$$

We have also from Newton's laws of motion for the bar

$$\rho\partial^2\xi/\partial t^2=-\partial Y_y/\partial y, \tag{28}$$

where ξ is the displacement of any point from its equilibrium position.

For a plated crystal the field E_x is constant along the length of the crystal, so that differentiating Eq. (26), we have

$$-\frac{\partial Y_y'}{\partial y}=\frac{1}{s_{22}'}\frac{\partial y_y'}{\partial y}+\frac{f_{14}(\partial P_x/\partial y)}{2c_{44}s_{22}'}$$

and

$$\frac{\partial P_x}{\partial y}=-\frac{f_{14}}{2c_{44}s_{22}'(\chi_{LC}+j\omega R)}\frac{\partial y_y}{\partial y}. \tag{29}$$

Eliminating $\partial P_x/\partial y$ we have

$$-\frac{\partial Y_y'}{\partial y}=\frac{1}{s_{22}'}\frac{\partial y_y'}{\partial y}\left[1-\frac{f_{14}^2}{4c_{44}^2s_{22}'}\left(\frac{1}{\chi_{LC}+j\omega R}\right)\right]$$

$$=\frac{1}{s_{22}'}\frac{\partial y_y'}{\partial y}(1-k^2), \tag{30}$$

where k the electromechanical coupling is complex because of the resistance associated with the inverse susceptibility χ_{LC}.

Since $y_y=\partial\xi/\partial y$ we have, finally,

$$\rho\frac{\partial^2\xi}{\partial t^2}=\frac{1}{s_{22}'}\frac{\partial^2\xi}{\partial y^2}(1-k^2). \tag{31}$$

For simple harmonic motion, this reduces to

$$0=\omega^2\xi+\frac{(1-k^2)}{\rho s_{22}'}\frac{\partial^2\xi}{\partial y^2}. \tag{32}$$

This complex equation is satisfied by

$$\xi=K_1\cosh(A+jB)y+K_2\sinh(A+jB)y, \tag{33}$$

provided that

$$\omega^2+(A+jB)^2(1-k^2)/\rho s_{22}'=0. \tag{34}$$

Introducing the value of $(1-k^2)$ from (30) and noting that

$$\chi_{LC}-f_{14}^2/4c_{44}^2s_{22}'=\chi_1-f_{14}^2/c_{44}=\chi_F, \tag{35}$$

we have, solving Eq. (34) for A and B

$$A=\omega(\rho s_{22}')^{\frac{1}{2}}\left\{\frac{-(\chi_F\chi_{LC}+\omega^2R^2)+[(\chi_{LC}^2+\omega^2R^2)(\chi_F^2+\omega^2R^2)]^{\frac{1}{2}}}{2(\chi_F^2+\omega^2R^2)}\right\}^{\frac{1}{2}}\doteq\omega(\rho s_{22}')^{\frac{1}{2}}\left(\frac{\chi_{LC}}{\chi_F}\right)^{\frac{1}{2}}\left[\frac{\omega R}{2\chi_{LC}}\left(\frac{\chi_{LC}}{\chi_F}-1\right)\right],$$

$$B=\omega(\rho s_{22}')^{\frac{1}{2}}\left\{\frac{(\chi_F\chi_{LC}+\omega^2R)+[(\chi_{LC}^2+\omega^2R^2)(\chi_F^2+\omega^2R^2)]^{\frac{1}{2}}}{2(\chi_F^2+\omega^2R^2)}\right\}^{\frac{1}{2}}\doteq\omega(\rho s_{22}')^{\frac{1}{2}}(\chi_{LC}/\chi_F)^{\frac{1}{2}}. \tag{36}$$

The approximate forms given are good provided $\omega R/\chi_{LC}$ and $\omega R/\chi_F<1$ which is usually the case.

We solve for the constants K_1 and K_2 of (33) in terms of the conditions existing when $y=0$. Then when $y=0$, $\sinh(A+jB)y=0$ and

$$K_1=\xi_1. \tag{37}$$

Similarly,

$$\partial\xi/\partial y=y_y=K_1(A+jB)\sinh(A+jB)y+K_2(A+jB)\cosh(A+jB)y. \tag{38}$$

Hence

$$K_2=\frac{y_{y_1}}{A+jB}=-\frac{1}{(A+jB)(1-k^2)}\left[Y_{y_1}'+\frac{f_{14}E_x}{2c_{44}s_{22}'(\chi_{LC}+j\omega R)}\right]s_{22}', \tag{39}$$

introducing the results of (26). Hence, using these values of K_1 and K_2 in Eqs. (33) and (38) and using the velocity

$$\dot{\xi}=j\omega\xi \tag{40}$$

in the equations we have the two relations

$$\begin{aligned}\dot{\xi}&=\dot{\xi}_1\cosh(A+jB)l_y-\left(\frac{s_{22}'}{\rho(1-k^2)}\right)^{\frac{1}{2}}\left[Y_{y_1}+\frac{f_{14}E_x}{2c_{44}s_{22}'(\chi_{LC}+j\omega R)}\right]\sinh(A+jB)l_y,\\ \left[Y_y+\frac{f_{14}E_x}{2c_{44}s_{22}'(\chi_{LC}+j\omega R)}\right]&=\left[Y_{y_1}+\frac{f_{14}E_x}{2c_{44}s_{22}'(\chi_{LC}+j\omega R)}\right]\cosh(A+jB)l_y\\ &\quad-\dot{\xi}_1(\rho(1-k^2)/s'_{22})^{\frac{1}{2}}\sinh(A+jB)l_y.\end{aligned} \tag{41}$$

To these equations we can add a third

$$Q=\frac{E_x}{4\pi}+P_x=E_x\left[\frac{1}{4\pi}+\frac{1}{\chi_{LC}+j\omega R}\right]-\frac{f_{14}y_y'}{2c_{44}s_{22}'(\chi_{LC}+j\omega R)}. \tag{42}$$

Integrating this with respect to y noting that $y_y'=\partial\xi/\partial y$, we have

$$Q_0=E_xl_yl_w\left[\frac{1}{4\pi}+\frac{1}{\chi_{LC}+j\omega R}\right]-\frac{f_{14}(\xi_2-\xi_1)l_w}{2c_{44}s_{22}'(\chi_{LC}+j\omega R)}, \tag{43}$$

where Q_0 is the total charge on the surface of width l_w. The current will be the time rate of change of the charge so that for the whole crystal we have

$$i=j\omega E\left(\frac{1}{4\pi}+\frac{1}{\chi_{LC}+j\omega R}\right)\frac{l_wl_y}{l_t}-\frac{f_{14}(\dot{\xi}_2-\dot{\xi}_1)l_w}{2c_{44}s_{22}'(\chi_{LC}+j\omega R)}, \tag{44}$$

where E is now the applied voltage since $E_x=E/l_t$. Equations (41) and (44) can be used to obtain the electrical impedance of a crystal for any mechanical terminating conditions.

To obtain the impedance of a fully plated crystal of length l_y, vibrating freely we set $Y_y=Y_{y_1}=0$ in Eq. (41) and solve for $\dot{\xi}_2$ and $\dot{\xi}_1$ obtaining

$$\dot{\xi}_1=-\dot{\xi}_2=\frac{f_{14}E_x\tanh(A+jB)l_y/2}{2c_{44}s_{22}'(\chi_{LC}+j\omega R)((1-k^2)/s_{22}')^{\frac{1}{2}}}. \tag{45}$$

Inserting these in (44) and collecting terms we have

$$Z=\frac{E}{i}=\left\{\frac{j\omega l_wl_y}{4\pi l_t}\left[1+\frac{4\pi}{\chi_{LC}+j\omega R}\times\left(1+\frac{k^2}{1-k^2}\frac{\tanh(A+jB)l_y/2}{(A+jB)l_y/2}\right)\right]\right\}^{-1}. \tag{46}$$

This impedance is equivalent to a capacitance $C_0=l_wl_y/4\pi l_t$ representing the capacitance between the plates if the crystal were absent, in parallel with a capacitance and resistance in series having an impedance equal to

$$(l_t/l_wl_y)[R-j\chi_{LC}/\omega] \tag{47}$$

and these in parallel with a third impedance

$$\frac{l_t}{j\omega l_wl_y}\left[(\chi_{LC}+j\omega R)\left(\frac{1-k^2}{k^2}\right)(A+jB)\frac{l_y}{2}\times\coth(A+jB)\frac{l_y}{2}\right]. \tag{48}$$

We are interested in the value of this impedance

near the resonant frequency which occurs when $Bl_y/2=\pi/2$. Introducing the approximation formulae for A and B given by (36) this impedance becomes

$$\frac{l_t}{l_w l_y}\left[\frac{\pi^2}{8}R+\frac{j}{\omega}\left(\frac{\chi_{LC}\chi_F}{\chi_{LC}-\chi_F}\right)\frac{\pi^2}{4}\frac{\Delta f}{f_R}\right], \tag{49}$$

where Δf is the difference in frequency between the actual frequency f and the resonant frequency f_R. Near the resonant frequency, this impedance is the same as that for a coil and condenser in series with a resistance which has the impedance.

$$R_E+(j/\omega C_E)[2\Delta f/f_R]. \tag{50}$$

Comparing (49) and (50) we have

$$\begin{aligned} R_E&=\frac{l_t}{l_w l_y}\frac{\pi^2}{8}R; \\ C_E&=\frac{2f_{14}^2 l_w l_y/l_t}{\pi^2 c_{44}^2 s_{22}'\chi_{LC}^2(1-f_{14}^2/4c_{44}^2 s_{22}'\chi_{LC})}; \\ L_E&=\frac{\rho\chi_{LC}^2(c_{44}^2 s_{22}'^2)l_t l_y/l_w}{2f_{14}^2}. \end{aligned} \tag{51}$$

At the resonant frequency, R_E is the value of this arm and since this resistance is very small compared to the shunting impedances of the other two arms, the impedance measured at the resonant frequency will be the resistance R_E.

If, now, we measure the electrical impedance of the crystal at twice the resonant frequency f_R, the impedance of (48) becomes very large and can be neglected compared to the other two arms. Furthermore due to the high dielectric constant of Rochelle salt, the impedance of C_0 is large compared to the second arm, and hence if we measure the impedance of the crystal at this frequency as was done on Fig. 6, we obtain the impedance

$$(l_t/l_w l_y)(R-j\chi_{LC}/\omega). \tag{47}$$

In the first section, a measurement was made of the elastic constants of a 45° X-cut crystal without plating. In order to determine what constants of the crystal will be measured for this case we can start with Eqs. (26) and (27) and impose the condition that Q, the charge on the surface, equal zero, or $E_x/4\pi=-P_x$. Introducing this relation in (26) and eliminating P_x we have

$$\begin{aligned} -Y_y'&=\frac{y_y'}{s_{22}'}-\frac{E_x f_{14}}{8\pi c_{44}s_{22}'}; \\ E_x\left[1+\frac{\chi_{LC}+j\omega R_1}{4\pi}\right]&=\frac{f_{14}y_y'}{2c_{44}s_{22}'} \end{aligned} \tag{52}$$

or eliminating E_x we have

$$\begin{aligned} -Y_y'&=\frac{y_y'}{s_{22}'}\left[1-\frac{f_{14}^2}{4c_{44}^2 s_{22}'(4\pi+\chi_{LC}+j\omega R)}\right] \\ &=\frac{y_y'}{s_{22}'}(1-k_B^2), \end{aligned} \tag{53}$$

where k_B is the coupling coefficient for the bare or unplated crystals. $s_{22}'/(1-k_B^2)$ is the complex compliance constant for the bare crystal which is somewhat different from the natural mechanical constant. Differentiating (53) with respect to y and substituting in (28) we can obtain the equations of motion for the bare crystal in the manner employed above. We find

$$\begin{aligned} \dot\xi&=\dot\xi_1\cosh(A_B+jB_B)l_y \\ &\quad -Y_y'\left(\frac{s_{22}'}{\rho(1-k_B^2)}\right)^{\frac12}\sinh(A_B+jB_B)l_y, \\ Y_y&=Y_{y1}\cosh(A_B+jB_B)l_y \\ &\quad -\dot\xi_1\left(\frac{\rho(1-k_B^2)}{s_{22}'}\right)^{\frac12}\sinh(A_B+jB_B)l_y, \end{aligned} \tag{54}$$

where

$$\begin{aligned} (A_B+jB_B)&=\left[\frac{-\omega^2\rho s_{22}'}{1-f_{14}^2/4c_{44}^2 s_{22}'(4\pi+\chi_{LC}+j\omega R)}\right]^{\frac12} \\ &\doteq\omega(\rho s_{22}')^{\frac12}\left(\frac{4\pi+\chi_{LC}}{4\pi+\chi_F}\right)^{\frac12} \\ &\quad\times\left[\frac{\omega R(f_{14}^2/4c_{44}^2 s_{22}')}{2(4\pi+\chi_F)(4\pi+\chi_{LC})}+j\right]. \end{aligned} \tag{55}$$

The method of measuring the impedance of the unplated bar employed in the second section in effect measures the impedance of a half-wavelength bar free to move on the far end. From (54) and (55) the impedance at the driven end near the

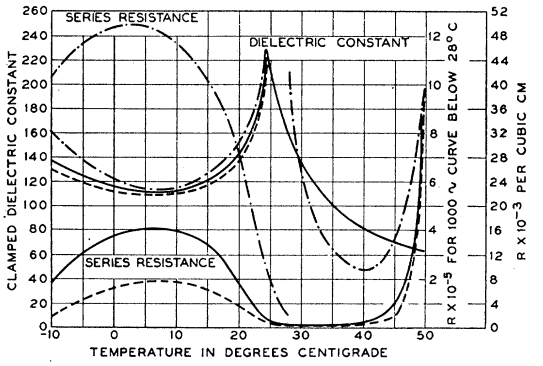

FIG. 7. Measurements of the clamped dielectric constant and associated series resistance of a 45° X-cut Rochelle salt crystal for three frequency ranges. Solid lines are measurements at 80 kc, dotted lines at 160 kc and dot-dash lines at 1000 cycles.

half-wave-length frequency is

$$R_M+jX_M=\left(\frac{\rho(1-k_B{}^2)}{s_{22}{}'}\right)^{\frac{1}{2}}\tanh(A_B+jB_B)l_y$$

$$\doteq\left(\frac{\rho(1-k_B{}^2)}{s_{22}{}'}\right)^{\frac{1}{2}}(\tanh A_Bl_y+j\tan B_Bl_y)$$

$$\doteq\left(\frac{\rho}{s_{22}}\right)^{\frac{1}{2}}l_wl_t\left[\pi\left(\frac{\omega R}{32\pi^2}\frac{f_{14}{}^2}{4c_{44}{}^2s_{22}{}'}+j\frac{\Delta f}{f_R}\right)\right]. \quad (56)$$

This corresponds to a series resistance, mass, and compliance having the values

$$R_M=\left(\frac{\rho}{s_{22}{}'}\right)^{\frac{1}{2}}l_wl_t\left(\frac{\omega R}{128\pi}\frac{f_{14}{}^2}{c_{44}{}^2s_{22}{}'}\right);$$

$$C_M=\frac{2s_{22}{}'l_y}{\pi^2l_wl_t};\quad L_M=\frac{\rho l_wl_tl_y}{2}. \quad (57)$$

The dissipation of the bar is usually defined by taking the ratio of the reactance of one of these elements to the resistance at the resonant frequency or

$$q=\frac{2\pi f_RL_M}{R_M}=\frac{32\pi c_{44}{}^2s_{22}{}'}{f_Rf_{14}{}^2},$$

and

$$f_R=\left(\frac{4\pi+\chi_F}{4\pi+\chi_{LC}}\right)^{\frac{1}{2}}\frac{1}{2l_y(\rho s_{22}{}')^{\frac{1}{2}}}. \quad (58)$$

In this equation, R must be expressed in c.g.s. electrostatic units rather than the practical units used on Fig. 6. This requires dividing the ohmic resistance by 9×10^{11}.

To see if this change in mechanical constants inherent in the polarization theory can account for the difference in the measured constants in the Curie region noted on Fig. 3, we see from (58) that the frequency constant for the bare crystal should be

$$f_R=\left(\frac{4\pi+\chi_F}{4\pi+\chi_{LC}}\right)^{\frac{1}{2}}f_M\doteq f_M\left[1-\frac{1}{8\pi}\left(\frac{f_{14}{}^2}{4c_{44}{}^2s_{22}{}'}\right)\right]. \quad (59)$$

All of the constants entering (59) depend very little on the temperature and show no appreciable change between the Curie points. From the values of the constants determined in a former paper,[1]

$$f_{14}=7.8\times10^4;\quad c_{44}=12.52\times10^{10};$$

$$s_{22}{}'=3.16\times10^{-12},$$

we have

$$f_R=f_M(1-0.00126). \quad (60)$$

That is, the resonant frequency f_R should be under the natural mechanical resonant frequency f_M by about 0.1 percent, and this value should be independent of the temperature. Hence the lowering in frequency between the Curie points must be due to an elastic change in the crystal. The same result is obtained for the ratio q of the reactance to resistance of the unplated crystal. At the temperature +5°C of the highest value of R, the q of the crystal if all of the dissipation were due to the dielectric loss would be

$$q=\frac{32\pi\times(12.52\times10^{10})^2\times3.16\times10^{-12}}{85{,}000\times16{,}000\times(7.8\times10^4)^2/9\times10^{11}}$$

$$=5.45\times10^5. \quad (61)$$

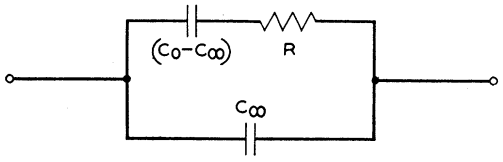

FIG. 8. Equivalent circuit for application of Debye's dielectric theory.

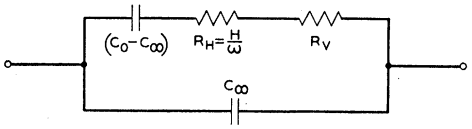

FIG. 9. Generalization of Debye's theory to include hysteresis resistance in one of the components.

This is considerably higher than the q measured at any temperature, and hence the q measured must have been due to the elastic properties of the crystal.

IV. Separation of Dielectric and Loss Components in the Clamped Dielectric Constant

At very low frequencies,[9] all measurements made indicate that the clamped dielectric constant rises to a high uniform value between the two Curie points and falls off outside this region. At higher frequencies, the clamped dielectric constant rises to a maximum at the two Curie points and falls off between them as shown by the solid line of Fig. 7. This was obtained from the data of Fig. 6 by using the Eq. (24).

$$\frac{4\pi}{K}\doteq\frac{4\pi}{K_{LC}}+\frac{f_{14}^2}{c_{44}}\left(\frac{s_{22}+s_{33}+2s_{23}}{1/c_{44}+s_{22}+s_{33}+2s_{33}}\right)$$
$$=\frac{4\pi}{K_{LC}}+0.0179, \quad (62)$$

inserting the measured values for these constants which are all nearly independent of the temperature. Following Debye's theory[10] of dielectric losses and dielectric constants, this divergence with frequency indicates that we are dealing with two or more dielectric sources in parallel.

Debye's theory considers the case of one dielectric source considered dissipationless, in parallel with another source which has in effect a series resistance of the viscous type as shown on Fig. 8. Combining these two sources, they have an impedance variation given by the equation

$$Z=\frac{-j}{\omega C_\infty}\left[1-\frac{(1-C_\infty/C_0)}{1+\omega^2\tau^2}+\frac{j\omega\tau(1-C_\infty/C_0)}{1+\omega^2\tau^2}\right], \quad (63)$$

where τ the relaxation time is given by

$$\tau=R(C_0-C_\infty)C_\infty/C_0. \quad (64)$$

At low frequencies the impedance will be that of the sum of the two capacitances whereas at high frequencies it will approach that of the capacitance C_∞. When the product of $\omega\tau$ is unity, the effective capacitance will be the mean of the two capacitances and the resistance will be a maximum and equal to

$$R=\frac{-j}{2\omega}\left(\frac{C_0-C_\infty}{C_0C_\infty}\right). \quad (65)$$

This theory cannot be applied directly to Rochelle salt since most of the resistance associated with the dielectric constant is of the hysteresis type which, according to Eq. (15), varies inversely as the frequency. The case of interest here is that shown on Fig. 9, where we have a capacitance (C_0-C_∞) in series with a hysteresis resistance (H/ω) and a viscosity resistance R_V, all shunted by a second capacitance C_∞. For this case the impedance measured as a function of frequency will be

$$Z=\frac{-j}{\omega C_\infty}\left[1-\frac{(1-C_\infty/C_0)[1+j(H\tau/R_V+\omega\tau)(1+H^2(C_0-C_\infty)^2C_\infty^2/C_0^2)]}{(1+2\omega H\tau^2/R_V+\omega^2\tau^2)(1+H^2(C_0-C_\infty)^2C_\infty^2/C_0^2)}\right] \quad (66)$$

where τ the relaxation time is now defined as

$$\tau=R_V\Big/\left(H^2+\frac{C_0^2}{C_\infty^2(C_0-C_\infty)^2}\right)^{\frac{1}{2}}. \quad (67)$$

In case $R_V=0$, the equation becomes

$$Z=\frac{-j}{\omega C_0}\left[1+\frac{H^2(C_0C_\infty)(1-C_\infty/C_0)^3+j(1-C_\infty/C_0)H}{1+H^2(1-C_\infty/C_0)^2C_\infty^2}\right] \quad (68)$$

[9] This is shown for example by the static measurement of Sawyer and Tower (Phys. Rev. **35**, 269 (1930)) and Bradford (B.S. Thesis, M. I. T., 1934) on the dielectric constant in the center of the hysteresis loop for a free crystal. Both measurements show a dielectric constant nearly independent of temperature between the Curie points. If this is interpreted according to (21) this indicates a constant clamped dielectric constant between the two Curie points.

[10] See P. Debye, *Polar Molecules* (Chemical Catalogue Co., New York, 1929); and E. J. Murphy and S. O. Morgan, "The dielectric properties of insulating materials," Bell Sys. Tech. J. **17**, 640 (1938).

and the capacitance remains constant while the effective resistance decreases inversely as the frequency.

In order to see if such a combination will account for the change in the dielectric constant noted, the clamped dielectric constant was determined at several frequency ranges. Figure 7 shows the clamped dielectric constant and the associated series resistance for the frequencies shown on Table I. The dielectric constant and series resistance was measured at twice this frequency by using the crystal whose dimensions are given on Table I and measuring the longitudinally clamped dielectric constant at twice the frequencies of Table I. The result is plotted on Fig. 7 by the dotted lines. As can be seen the dielectric constant is somewhat smaller and the resistance is about half as large. Another measurement at 1000 cycles was obtained by using the measurement of Dr. G. T. Kohman on the dielectric constant and associated dielectric losses for a Rochelle salt crystal free to vibrate. The clamped dielectric constant was obtained from the equation

$$\frac{4\pi}{K}=\frac{4\pi}{K_F}+f_{14}^2/c_{44}=\frac{4\pi}{K_F}+0.0485, \qquad (21)$$

introducing the measured values for f_{14} and c_{44}. The resistance measured was unchanged since from Eq. (21) the same resistance should be measured for a free or clamped crystal.

Above the Curie point the coincidence of all the measurements of the dielectric constants indicate that the viscous resistances are negligible. Up to 40°C most of the dissipation is due to a hysteresis type resistance as shown by the fact that the measured resistance varies nearly inversely as the frequency. Above 40° the effect of an ohmic shunt resistance is felt due to the leakage properties of the crystal near the melting point. At the Curie point the viscous resistance is still small and the clamped dielectric constant attains nearly its full value. When the temperature is between the Curie points the effect of the viscous resistance on one of the components becomes larger and as a result the dielectric constant approaches that of one component only. At 4°C, this value is nearly reached as is shown by the fact that the dielectric constants measured at 1000 cycles, 84,000 cycles and 168,000 cycles are very nearly the same. The resistance associated with this component is nearly all hysteresis, as is shown by the fact that the series resistance is nearly inversely proportional to the frequency. While the data are not sufficient to give an accurate evaluation of the dielectric constants and associated resistances it indicates that we are dealing with two dielectric components which are nearly constant with temperature between the two Curie points. The one having little viscous resistance associated with it has a dielectric constant of about 100, while the other has a dielectric constant of 140. The relaxation time of the second component is quite large except near the Curie points since the dielectric constant of the first component is nearly attained at 1000 cycles.

Since viscous resistance is usually associated with a rotation of molecules, it seems likely that the second dielectric component is due to the dipoles of the Rochelle salt. The first component which has little viscous resistance is probably due to the displacements of the ions in the lattice. Since at optical frequencies the dielectric constant is in the order of 2.5 there must be some viscous resistance associated with the ion displacements, and another component having a much lower dielectric constant. This component, however, will not be measured for any radiofrequencies,[11] and very high frequency measurements will, in all probability, measure only the dielectric constant due to the ion displacements. Both components are increased between the Curie points and both components have hysteresis effects, indicating a cooperative action of the molecules.

[11] W. Bantle and G. Busch, Helv. Phys. Acta **10**, 262 (1937) find that up to frequencies of 7.5×10^8 cycles the dielectric constant does not get below 100.